Advection-Induced Spectrotemporal Defects in a Free-Electron Laser

S. Bielawski and C. Szwaj

Laboratoire de Physique des Lasers, Atomes et Molécules, UMR CNRS 8523, Centre d'Études et de Recherches Lasers et Applications, FR CNRS 2416, Université des Sciences et Technologies de Lille, F-59655 Villeneuve d'Ascq Cedex, France

C. Bruni, D. Garzella, G. L. Orlandi, and M. E. Couprie

CEA/DSM/DRECAM/SPAM, Bâtiment 522, 91191 Gif-sur-Yvette, France and Laboratoire pour l'utilisation du rayonnement électromagnétique, Bâtiment 209D, Université Paris Sud, BP34, 91898 Orsay Cedex, France

(Received 30 November 2004; published 14 July 2005)

We evidence numerically and experimentally that advection can induce spectrotemporal defects in a system presenting a localized structure. Those defects in the spectrum are associated with the breakings induced by the drift of the localized solution. The results are based on simulations and experiments performed on the super-ACO free-electron laser. However, we show that this instability can be generalized using a real Ginzburg-Landau equation with (i) advection and (ii) a finite-size supercritical region.

DOI: 10.1103/PhysRevLett.95.034801 PACS numbers: 41.60.Cr, 05.45.−a, 42.65.Sf

Stationary wave formation is generically subjected to drift phenomena when the reflection symmetry is broken. Increasing a parameter v, controlling the drift velocity from zero, leads to phenomena associated with known subtle issues, such as pinning at the boundaries [1], the distinction between convective and absolute instabilities [2], and the so-called noise-sustained structures [3]. These behaviors have been extensively studied in pattern-forming systems [4–6] with local coupling (diffusion and dispersion), and when the wave solution is not localized.

However, less is known on drift effects in slightly more complex situations, in particular, when the wave formation is localized in a region of space because of spatial ramps and/or when the coupling is different from the elementary diffusion and dispersion, e.g., global coupling. Such situations appear in different contexts such as in hydrodynamics [7], chemistry [8], gas discharge physics [9], optics [10–12], or biology [13].

In this Letter, we consider the effect of advection in a system with a localized solution, and focus on the first regimes appearing when the drift velocity parameter is increased. We start with the numerical and experimental study of a free-electron laser (FEL) [14,15], in which the relevant wave pattern is the longitudinal field distribution of a picosecond optical pulse that experiences round-trips between two mirrors. We first show numerically that a representation of the dynamics in Fourier space reveals hidden aspects of the dynamics: While in direct space we observe the classical drifts and noise-sustained structures, a representation of the dynamics in Fourier space reveals spatiotemporal dislocations similar to the ones observed in the Eckhaus instability [5,16]. Then we support these predictions with experiments on the super-ACO storage-ring FEL [17]. Finally, we study two elementary model equations to show that these phenomena can appear in a large class of systems.

A FEL oscillator is a pulsed laser source whose amplifying media is a relativistic electron beam traveling through a region of periodic permanent magnetic field [15]. Besides their present and potential applications at various wavelengths (from infrared to UV/X), FELs display a rich variety of spatiotemporal instabilities [17,18]. The dynamics is strongly affected by the synchronism between the round-trips of the laser pulse and the electron bunch [Fig. 1(a)]. The evolution of a pulse in such a cavity obeys the well-known *Haus master equation* commonly used for mode-locked lasers [11,19–21], and established independently for FELs [22,23]. Haus-type models basically de-

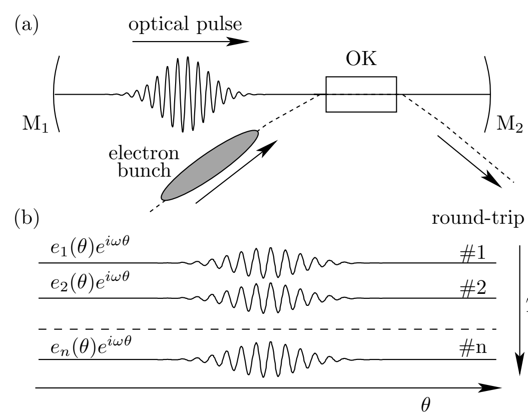

FIG. 1. (a) Experimental setup for a storage-ring FEL. The wave is constituted of the optical pulse (several picoseconds duration) that experiences round-trips between two mirrors M_1 and M_2. At each passage the pulse is amplified by the interaction with the relativistic electron bunch of a storage ring (several tens of picoseconds, energy in the GeV domain) in an optical klystron (OK), see Refs. [22,23] for details. (b) Illustration of the theoretical framework: One considers the complex envelope profile $e_n(\theta)$ of the field pattern at each electron passage, and takes the continuous limit $n \to T$.

scribe the evolution of the successive complex envelopes of field profiles $e_n(\theta)$ (with θ defined by $\theta = z/c$ and z the longitudinal coordinate of the pulse) at each round-trip n. Here, the series $e_n(\theta)$ is taken in synchrony with the electron bunch passage [see Fig. 1(b)]. We are thus in the presence of a spatiotemporal system for which the relevant space is θ, and the relevant time is the round-trip number n. The continuous limit is taken, so that we transform the discrete time n into a continuous "slow time" T [19]. The evolution of $e(\theta, T)$ obeys the adimensional equation

$$e_T + v e_\theta = -e + g(T) f(\theta)(e + e_{\theta\theta}) + \sqrt{\eta}\xi, \quad (1)$$

where the slow time T associated with the round-trips is expressed in units of the field cavity lifetime τ_c (typically in the microsecond range). The fast time θ resolving the pulse shape is expressed in units of $t_u = \pi/(\sqrt{2}\Delta\omega_g)$ (in the subpicosecond range) with $\Delta\omega_g$ the gain width of the operating line [24]. Physically the diffusion operator accounts for the finite linewidth of the gain [19], and a first derivative operator (not essential for our purpose) can also be taken into account [25]. v expresses the mismatch between the period of the electron bunch passages T_e and the laser cavity round-trip time T_L: $v = \frac{T_L - T_e}{T_L} \frac{\tau_c}{t_U}$. v plays the role of an advection velocity (in units of t_U/τ_c) and is the main control parameter of the FEL. $f(\theta) = \exp(-\theta^2/2\sigma_b^2)$ characterizes the gain shape due to the electron bunch longitudinal distribution, where σ_b is the bunch duration in units of t_u. The effect of spontaneous emission is taken into account by the white noise term $\xi(\theta, T)$ with $\langle \xi^*(\theta', T')\xi(\theta, T)\rangle = \delta(\theta - \theta')\delta(T - T')$. The level of noise is controlled by the parameter η, which is purely phenomenological. The gain dynamics $g(T)$ depends on the precise accelerator and insertion device. A simple expression for a storage ring can be written in adimensional units as [18,26]

$$g(T) = \frac{A}{\sigma(T)} \exp[-(\sigma^2(T) - 1)/2], \quad (2)$$

$$\frac{d\sigma^2}{dT} = \frac{1}{T_s}\left(1 - \sigma^2 + \int_0^L |e(\theta, T)|^2 d\theta\right). \quad (3)$$

Equation (2) links the gain g to the heating variable σ, which is the rms width of the electron energy distribution in units of its value without laser emission. A is the maximum gain in units of the cavity losses (laser operation requires $A > 1$). Equation (3) accounts for the relaxation of σ^2, and the bunch heating by the laser which provides the gain saturation process. The heating relaxation time T_s is equal to the synchrotron damping time in units of the field cavity lifetime ($T_s \gg 1$). L is the round-trip time in units of t_u. In the following, we use typical parameters corresponding to the super-ACO FEL: $1/T_s = 0.0047$, $\sigma_b = 862$, $A = 4.5$, $t_u = 80$ fs, $\eta = 3.3 \times 10^{-10}$. The unit of T is $\tau_c = 40\ \mu$s.

The different regimes observed when the drift parameter v is increased are represented in Fig. 2. In a small range near $v = 0$, the solution is a stable pulse [Fig. 2(a)]. The first instability occurs for $v = \pm 0.15$ here. Beyond this value the solution is a localized structure that drifts slowly, breaks, and is replaced recurrently by another one [Fig. 2(d)]. The breakings appear more frequently with increasing value of v [Fig. 2(g)]. At large values [Fig. 2(j)], the solution is a noise-sustained structure, similar to the one studied by Morgner and Mitschke and by Geddes *et al.* in actively mode-locked lasers [10,11], and characterized by an extreme sensitivity to noise.

We concentrate here on the regimes occurring just above the first transition in order to find the instability mechanism. In our approach, we take a different point of view and examine the pattern in Fourier space $\tilde{e}(k, T)$. Indeed, integration of the FEL model with various parameters reveals that the drift instability induced by the advection term (the

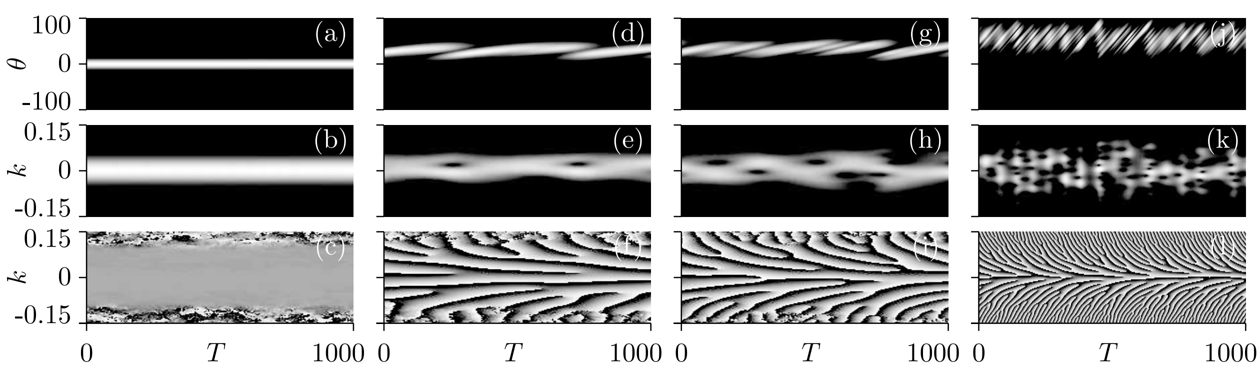

FIG. 2. Numerical solution of the FEL model (1–3) versus the drift parameter v. The first line (a),(d),(g),(j) represents the pulse shapes versus time $|e(\theta, T)|^2$. The evolutions of the spatial Fourier transforms $\tilde{e}(k, T)$ are represented below each regime: The second and third lines (b),(e),(h),(k) and (c),(f),(i),(l) represent the associated amplitudes $|\tilde{e}(k, T)|^2$ and phases $\arg[\tilde{e}(k, T)]$ associated with (a),(d),(g),(j), respectively. The drift velocity increases from left to right: First column (a),(b),(c): $v = 0$, below the instability threshold; second column (d),(e),(f): $v = 0.5$, moderately above the threshold; third column (g),(h),(i): $v = 0.7$; fourth column (j),(k),(l): $v = 3.4$, a typical noise-sustained structure observed at high drift velocity. $T = 1000$ corresponds to 20 ms, and $\theta = 100$ to 8.3 ps. Note that the holes present in the spectrum evolutions are associated with zeroes of the field.

breaking of the localized solution) is systematically associated with the appearance of defects in the spectrotemporal evolution. These are characterized by holes in the amplitude distribution $|\tilde{e}(k,T)|$ [Figs. 2(e), 2(h), and 2(k)], associated with phase singularities [Figs. 2(f), 2(i), and 2(l)]. These regimes seem similar to the phase-slips regimes occurring, e.g., in the ramp-induced Eckhaus instabilities [16,27]; i.e., however, at this point, no conclusion can be inferred. In addition, the presence of this instability could explain the fact that the mean value of the width of both the pulse and its spectrum increase with the drift v, as it has been reported in FEL experiments [28].

In order to verify that these predictions correspond to observable experimental behaviors, we have performed a spectrotemporal analysis of the super-ACO UV FEL (350 nm) at Orsay. The recordings in direct space of $|e(\theta,T)|^2$ have been performed using a double sweep streak camera (Hamamatsu C5680). The spectrochronograms $|\tilde{e}(k,T)|^2$ are obtained using a plane Fabry-Perot etalon (finesse 60, free spectral range 300 GHz) in convergent light followed by a CCD LineScan camera (128 pixels, 33 000 lines/s). The streak camera and spectrum recordings are presented in Fig. 3 for four typical parameters. The drift parameter v is directly controlled by the fundamental frequency of the rf accelerating fields (≈ 100 MHz). The storage ring operated with two 80 ps long bunches (rms) at 800 MeV, with a current in the 30–50 mA range.

First, as usual in FEL oscillators [29], we observe in a small region near zero detuning a regime associated with a single stable pulse [Fig. 3(a)]. When the detuning exceeds a threshold value (in the Hertz range), we observe a transition leading to a drift of the structure [Figs. 3(b) and 3(c)] in either direction, depending on the sign of the detuning. For large detuning values, the system exhibits noise-sustained structures [Fig. 3(d)]. We find that the spectrochronograms display the appearance of zero-intensity holes [Figs. 3(e)–3(g)] as predicted numerically.

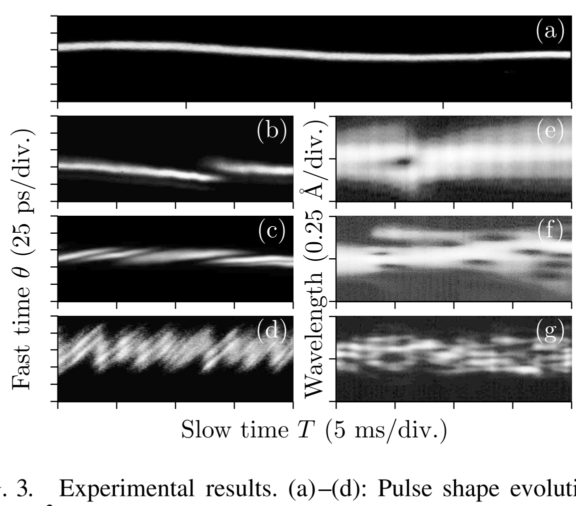

FIG. 3. Experimental results. (a)–(d): Pulse shape evolutions $|e(\theta,T)|^2$ recorded with a streak camera. (e)–(g): Optical spectrum evolutions $|\tilde{e}(k,T)|^2$ associated with (b)–(d) (the parameters are identical, but spectra and streak recordings are not synchronized). (a): case of rf frequency ν_0 associated to almost perfect synchronism (i.e., $v \approx 0$); (b),(e): case of rf frequency slightly just beyond the lower instability threshold ($\nu_0 -$ 0.5 Hz); (c),(f): case of rf frequency well beyond the upper instability threshold ($\nu_0 +$ 1.5 Hz); (d),(g): noise-sustained structure observed far from the instability threshold ($\nu_0 +$ 3 Hz).

At this point, numerical and experimental results reveal that the present behavior has a dual character. Indeed, (i) it appears in direct space in the form of an advection-induced drift instability, (ii) it is characterized in Fourier space by the presence of defects and presents the characteristic features of a ramp-induced Eckhaus instability. In a next step, one may wonder whether this phenomenon is likely to occur in other systems, or is a unique consequence of the FELs' physical details. To know more precisely the conditions required, we have studied the real Ginzburg-Landau with a slow parabolic spatial gain dependence that ensures the occurrence of a localized solution. We have considered both cases of gain saturation by local and global coupling:

$$e_T + ve_z = e_{zz} + R(1 - \epsilon^2 z^2)e - S + \sqrt{\eta}\xi, \tag{4}$$

with

$$S = |e|^2 e \tag{5}$$

or

$$S = e\int_{-\infty}^{+\infty} |e|^2 dz, \tag{6}$$

and $\epsilon \ll 1$. The value of ϵ has been varied in a wide range keeping an order of magnitude leading to the same typical pulse width as in the FEL case.

These model equations have been integrated for various values of the control parameters (v, ϵ, R). We found that all the features discussed below are reproduced beyond some threshold for v (see Fig. 4). This shows that we can expect the present phenomenon to occur in a range of systems either with global and local saturation coupling, provided

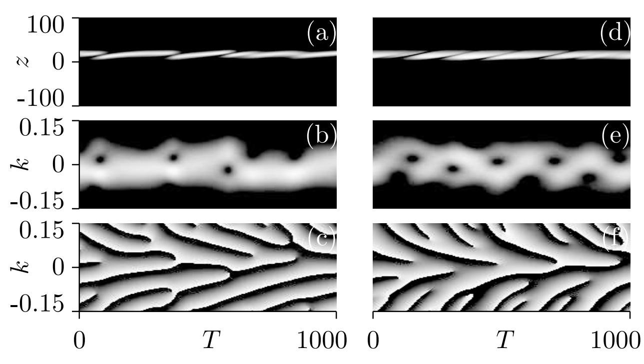

FIG. 4. Numerical integration of the Ginzburg-Landau equation with ramps and advection (4). (a)–(c): case of global coupling [S given by Eq. (6)], $v = 0.6$, $\epsilon = .0012$, $R = 4$. (d)–(f): case of local coupling [S given by Eq. (5)], $v = 0.6$, $\epsilon = 0.01$, $R = 0.04$. (a),(d) represent $|e(z,T)|$, (b),(e): $|\tilde{e}(k,T)|$, (c),(f): $\arg[\tilde{e}(k,T)]$.

they display advection and a solution localized by the presence of parameter ramps. Let us finally emphasize that the other features very peculiar to FELs and lasers in general (as the slow time scale T_s of the saturation dynamics), though complicating the modeling, do not appear to be essential.

Finally, let us remark that we can obtain insights on the origin of the spectrotemporal dislocations by examining the evolution equation for the Fourier transform $\tilde{e}(k, T)$ of $e(z, T)$ in the case of global coupling. The Fourier transform of Eqs. (4) and (6) is:

$$\tilde{e}_T = \rho(k)\tilde{e} + \epsilon^2 R \tilde{e}_{kk} - \tilde{e}\int_{-\infty}^{+\infty} |\tilde{e}|^2 dk + \sqrt{\eta}\zeta, \qquad (7)$$

with $\langle \zeta^*(k', T')\zeta(k, T)\rangle = \delta(k - k')\delta(T - T')$ and $\rho(k) = (R - k^2 - i v k)$. This is a Ginzburg-Landau equation without advection, and with a control parameter $\rho(k)$ that varies *slowly* in space (with respect to the small diffusion length $\epsilon\sqrt{R}$).

Equation (7) can be viewed as describing a chain of oscillators with natural frequencies $\omega(k) = -vk$. This dependence of ω on k causes a frustration that is expected to lead to a desynchronization of the chain through the appearance of phase slips at a threshold value of v. In addition, the situation presents similarities with the so-called *ramp-induced Eckhaus instability* [16] observed in hydrodynamics [16,30] and in lasers [27]. In both cases, the dynamics is governed by the spatial evolution of a control parameter $\rho(k)$, and the instability is characterized by the occurrence of phase slips. However, further work is needed to conclude on the precise links between the instability mechanism considered here and the ramp-induced Eckhaus instability. Since the nonlocal saturation notably complicates the required perturbative analysis, we leave the detailed analytical work and analytical determination of the transition point (through, e.g., the derivation of a phase-diffusion equation [16,30]) to further studies.

In conclusion, localized systems with advection can display an instability characterized simultaneously by a drift instability in direct space and a defect instability in Fourier space, similar to the Eckhaus instability. The instability occurs at advection velocities much smaller that the ones leading to noise-sustained structures. The signature in the FEL experiment performed here is the presence of holes (intensity zeros) in the spectrotemporal diagrams. Preliminary studies of the modified Ginzburg-Landau equation (4) shows that this phenomenon is expected to affect a range of systems displaying localized solutions with either local or global coupling. Future works concerns the study of the precise respective roles of the steady-state instabilities (in the sense of *bifurcations*) and the hypersensitivity to noise due to the non-normal operators involved in the dynamics [10,11,31].

The CERLA is supported by the Ministère chargé de la Recherche, the Région Nord-Pas de Calais, and the FEDER.

[1] P. Kolodner, Phys. Rev. E **48**, R4187 (1993).
[2] P. Huerre and P. A. Monkewitz, Annu. Rev. Fluid Mech. **22**, 473 (1990).
[3] R. J. Deissler, Physica D (Amsterdam) **25**, 233 (1987).
[4] K. L. Babcock, G. Ahlers, and D. S. Cannell, Phys. Rev. E **50**, 3670 (1994).
[5] M. C. Cross and P. C. Hohenberg, Rev. Mod. Phys. **65**, 851 (1993).
[6] E. Louvergneaux, C. Szwaj, G. Agez, P. Glorieux, and M. Taki, Phys. Rev. Lett. **92**, 043901 (2004).
[7] F. Hayot and Y. Pomeau, Phys. Rev. E **50**, 2019 (1994).
[8] V. K. Vanag, Y. Lingfa, M. Dolnik, A. M. Zhabotinsky, and I. R. Epstein, Nature (London) **406**, 389 (2000).
[9] B. Bruhn, B.-P. Koch, and P. Jonas, Phys. Rev. E **58**, 3793 (1998).
[10] U. Morgner and F. Mitschke, Phys. Rev. E **58**, 187 (1998).
[11] J. B. Geddes, W. J. Firth, and K. Black, SIAM J. Appl. Dyn. Syst. **2**, 647 (2003).
[12] S. Coen, M. Tlidi, P. Emplit, and M. Haelterman, Phys. Rev. Lett. **83**, 2328 (1999).
[13] J. von Hardenberg, E. Meron, M. Shachak, and Y. Zarmi, Phys. Rev. Lett. **87**, 198101 (2001).
[14] M. Billardon *et al.*, Phys. Rev. Lett. **51**, 1652 (1983).
[15] G. Dattoli, A. Renieri, and A. Torre, *Lectures on the Free Electron Laser and Related Topics* (World Scientific, Singapore, 1993).
[16] H. Riecke and H.-G. Paap, Phys. Rev. Lett. **59**, 2570 (1987).
[17] G. De Ninno, D. Nutarelli, D. Garzella, and M. E. Couprie, Phys. Rev. E **65**, 056504 (2002).
[18] G. De Ninno, D. Fanelli, C. Bruni, and M.-E. Couprie, Eur. Phys. J. D **22**, 269 (2003).
[19] H. A. Haus, IEEE J. Quantum Electron. **11**, 323 (1975).
[20] A. M. Dunlop, W. J. Firth, D. R. Heatley, and E. M. Wright, Opt. Lett. **21**, 770 (1996).
[21] N. Joly and S. Bielawski, Opt. Lett. **26**, 692 (2001).
[22] P. Elleaume, IEEE J. Quantum Electron. **21**, 1012 (1985).
[23] G. Dattoli, T. Hermsen, A. Renieri, A. Torre, and Gallardo, Phys. Rev. A **37**, 4326 (1988).
[24] More precisely, the spontaneous emission spectrum and the gain spectrum of an optical klystron are typically oscillatory. $\Delta\omega_g$ is half the period of this oscillation.
[25] In fact the refraction index associated with the gain medium [19,23] (lethargy) adds a term $\alpha g(T) f(\theta)\partial_\theta e$. This latter is neglected because it is not found to affect significantly the results (only a shift of the bifurcation points in v by αv) for the parameters considered here.
[26] S. Bielawski, C. Bruni, G. L. Orlandi, D. Garzella, and M. E. Couprie, Phys. Rev. E **69**, 045502(R) (2004).
[27] J. Plumecoq, C. Szwaj, D. Derozier, M. Lefranc, and S. Bielawski, Phys. Rev. A **64**, 061801(R) (2001).
[28] K. Kimura, J. Yamazaki, S. Takano, T. Kinoshita, and H. Hama, Nucl. Instrum. Methods Phys. Res., Sect. A **375**, 62 (1996).
[29] R. Roux *et al.*, Nucl. Instrum. Methods Phys. Res., Sect. A **393**, 33 (1997).
[30] H.-G. Paap and H. Riecke, Phys. Fluids A **3**, 1519 (1991).
[31] F. X. Kärtner, D. M. Zumbühl, and N. Matuschek, Phys. Rev. Lett. **82**, 4428 (1999).